NEURAL CORRELATES OF ELBOW JOINT KINEMATIC VARIABILITY

by

GAUTAM SIDDARTH NATARAJAN

A thesis submitted to the

Graduate School – New Brunswick

Rutgers, The State University of New Jersey

and

The Graduate School of Biomedical Sciences

University of Medicine and Dentistry of New Jersey

in partial fulfillment of the requirements

for the degree of

Master of Science

Graduate Program of Biomedical Engineering

Written under the direction of

William Craelius, PhD

and approved by

_____

_____

_____

New Brunswick, New Jersey

October 2009

ABSTRACT OF THE THESIS

Neural correlates of elbow joint kinematic variability

By Gautam Siddarth Natarajan

Thesis Director:

William Craelius, PhD

A fundamental tenet of motor control is that point-to-point reaching motions follow an approximately straight line trajectory with a bell-shaped velocity profile. However, these abstractions are not universally observed. Previous work in our lab revealed that most spatiotemporal elbow trajectories do not necessarily conform to a straight-line, which is believed to be 'natural' human motion. Instead, spatiotemporal trajectories are best characterized by a small set of simple, analytic functions including both linear and non-linear waveforms. Here, I suggest that the differences observed in elbow kinematics are a direct consequence of varying motor planning, which is represented by the electromyography (EMG).

Fourteen healthy subjects were asked to perform several self-paced, untargeted elbow articulations that maximize smoothness within a comfortable range of motion; EMG of the biceps and kinematic traces were recorded simultaneously. Kinematic traces were modeled by a set of simple, monotonic functions, while EMG traces were reconstructed by parabolic waveforms, via a parameterized curve-fitting method. EMG traces (r-EMG) and their parabolic reconstructions (p-EMG) were used independently to

predict adherence to each of 3 kinematic types. It was hypothesized that the p-EMG and r-EMG from the kinematic adherence group ($r^2 > 0.9979$) would exhibit statistical and parametric differences from the departure group ($r^2 < 0.9951$) of the same kinematic type.

Both r-EMG and p-EMG were useful in predicting adherence to global kinematic morphology with high sensitivity and specificity across subjects. Coupling the substantial predictive value and the similar information content (87.80% of the decisions were identical) of both EMG modalities implied that p-EMG can be used as a simple, informative approximant of r-EMG of the biceps during self-paced, untargeted elbow flexions. The features selected for classification were robust across subjects along with the predictive value, suggesting there is degeneracy in the neural command. Degeneracy in the neural command matches the widespread observation of highly stereotyped kinematics. Elbow trajectories most commonly adhered to sigmoid morphology. Future work should develop a comprehensive depiction of the neural control of voluntary movements.

Dedication

This thesis is dedicated to my family. Their love and support inspire me to achieve the impossible.

Table of Contents

List of Tables

List of Illustrations

Section 1. INTRODUCTION

Human motor control involves an intricate transduction of neural information into a muscular contraction. The immense complexity of movement coordination is generalized by the *degrees of freedom* problem: how does the central nervous system (CNS) coordinate several components to produce highly stereotyped motions [Bernstein 1967]? Since the advent of the degrees of freedom problem, numerous studies investigating motor control have been published. Nevertheless, there remains an abundance of ambiguities in our understanding of motor control, which the Defense Advanced Research Projects Agency (DARPA) has made a top priority by substantially increasing their budget aimed at completing our quest of understanding the biomechanical and bioelectric aspects of motor control [Ade 2009].

Neural command of the musculature is routinely quantified by electromyography (EMG), which is an electric recording of action potentials spreading through the tissue. Typical surface EMG acquisition involves placing electrodes on the surface of the skin. The signal's noninvasive acquisition makes it the primary modality of representing muscle activation. Consequently, thorough comprehension of the EMG is crucial to resolving the robustness of the motor system.

EMG has been used extensively as an input signal to muscle models, which aim to predict the force generated by a muscle [Camilleri & Hull 2005; Koo & Mak 2005; Raasch et al. 1997; Neptune & Hull 1998]. Due to its notoriously stochastic nature, investigators proceeded to use EMG models to approximate the raw signal by simple waveforms; sloped waveforms are more accurate representations of EMG and better

predictors of muscle force than rectangular waveforms [Camilleri & Hull 2006]. Thus far, EMG has been investigated by experimental protocols involving isometric contractions, ballistic motions, or tracked paradigms [Doheny et al. 2008; Gabriel 2007; Wrbaskic & Dowling 2006; Clancy & Hogan 1997]. Each of these motions involves the generation of an EMG signal that has a large departure from baseline voltage. Therefore, the signal to noise ratio (SNR) is relatively high, and the signal is conducive to subsequent analyses. EMG analyses have focused on the neural command of large tensile forces generated by specific muscle groups; there is a dearth of information on the EMG of self-paced elbow articulations. Consequently, muscle models have yet to accurately predict kinematics during self-paced elbow flexions without resistance [Koo & Mak 2005]. Studying EMG during self-paced, untargeted motions is significant because neural recruitment and muscle activation is thought to be a function of the hand's position in the extracorporeal space [Georgopoulos 1981; Morasso 1981; Abend et al. 1982], whereas typical experimental motions (isometric, ballistic, or tracked paradigms) may be governed by altered central signals [Suzuki & Yamazaki 2005].

Hand pathways during 3-D reaching tasks are generally considered to traverse approximately straight line trajectories and are characterized by a highly stereotyped bell-shaped velocity profile [Flash & Hogan 1985]. The overwhelming complexity of multi-joint movements spawned the examination of single joint trajectories (SJTs), where movement is constrained to a specific joint. Isolated elbow articulations have also been observed to conform to the bell-shaped velocity profile [Rohrer et al. 2002]. This generalization of linear spatiotemporal trajectories is approximately true on average,

however there is evidence suggesting individual repetitions may deviate significantly from this trajectory type and may exhibit stochastic variability. In the Rutgers University Rehabilitation Laboratory, it has been found that individuals doing multiple repetitions select from a set of 6 statistically independent archetypical waveforms, 5 of which are non-linear [Wininger et al. 2009]. Given this repertoire of kinematic types, the question arises as to what determines the morphology of elbow flexions. Specifically, are they a result of musculoskeletal dynamics, or do they reflect variations in central motor planning?

Morphological differences between kinematic traces should be rooted in the neural command. However, this has never been verified because of the difficulty in interpreting EMG from self-paced elbow flexions. Correlating the EMG to the kinematic morphology would greatly improve our current understanding of motor control. Herein, I examine the early phase of EMG during self-paced elbow articulations in an attempt to…

1. Predict kinematic morphology from EMG.
2. Examine the similarity of EMG waves and their parabolic reconstructions.
3. Determine comparable motor characteristics across subjects.

Section 2. METHODS

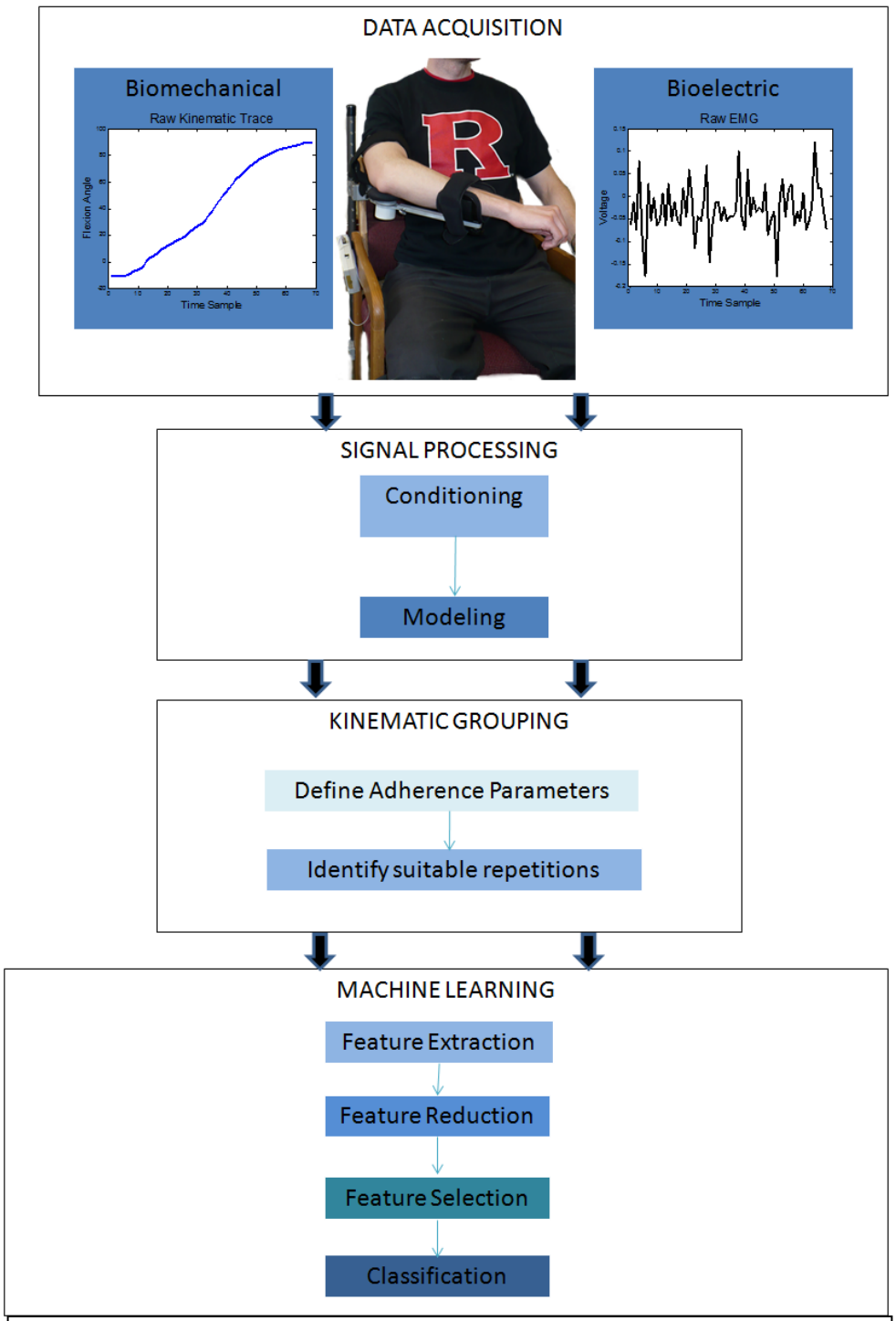

Figure 1: Methods Overview – Research methods can be compartmentalized into four discrete sections, where the output of each compartment is the input for the subsequent compartment.

A. Data Acquisition

Fourteen right-hand dominant (RHD) healthy volunteers [9 male, 5 female] with no history of neural or orthopedic impairments were recruited to participate in this study. Subjects provided written informed consent, and the study was conducted within the parameters approved by the Rutgers University IRB.

Subjects were seated comfortably in the MAST, which isolates upper limb motion to elbow articulations in the horizontal plane. The right elbow rested in the plane of the potentiometer to ensure accurate recording of anatomic flexion angle. As a subject performed practice flexions, the biceps were probed for the most robust bioelectric signal. The electrode was firmly secured to the biceps with medical tape and a Velcro strap. Arm straps on the MAST were then secured. Subjects performed several articulations at the elbow while kinematic and myoelectric data were recorded after receiving the following instructions:

> *Move as smoothly as you can at a comfortable pace. Flex and extend through you're maximal range of motion without hyperextending at the elbow.*

Exercises terminated before fatigue set in.

EMG and kinematic time-courses were sampled at 80 Hz and collected with a data acquisition board (USB 6008, National Instruments, Austin, TX). A VI developed in LabVIEW (National Instruments, Austin, TX) collected the streaming data and wrote it to a common file that is readily opened in MATLAB (Mathworks, Natick, MA) and

Microsoft Excel. Datasets were truncated by removing the first and last few repetitions to account for edge effects.

B. Signal Processing

B.1. Conditioning

Kinematic data were low-pass filtered at a cut-off frequency of 5 Hz with a second order Butterworth filter [Feng & Mak 1997]. Raw EMGs were band-pass filtered between 7.5 and 15 Hz by a fourth-order Butterworth filter and full-wave rectified. Full-wave conditioning was complete after imposing a 7 point moving average on the EMG [Koo & Mak 2005]. Since ensuing analyses were to be performed on individual elbow flexions, the datasets had to be parsed into individual repetitions. A single flexion is an elbow articulation that begins with the arm at full extension and finishing when the hand is closest to the subject's chest. The graphical analog of a flexion is marked by the time-course between angular minima and maxima. Flexion endpoints were determined by inputting a pre-defined angular threshold and perusing above and below the threshold until the minima and maxima were identified.

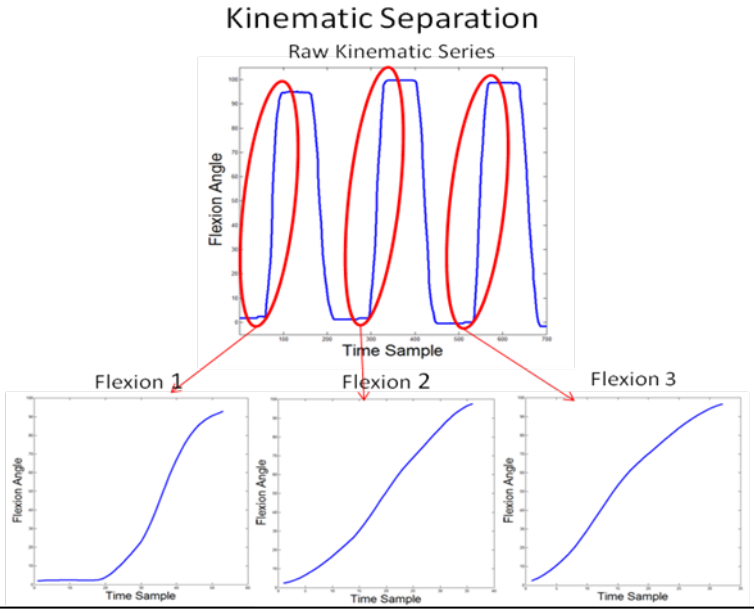

Figure 2: Kinematic Separation – Kinematic data are recorded as a single time series and subsequently separated into individual motions.

One-to-one time point correspondence was maintained between kinematic and EMG data by separating the bioelectric signal synchronously with the kinematic data. Simultaneous examination of the time-course of EMG and kinematics revealed a sharp increase in biceps EMG voltage in the regional domain near full flexion. This spatial dependence of EMG suggests there is increased biceps activity near full flexion. For my purposes, investigating this rise in voltage was not of primary importance because the majority of the workspace was already traversed by the onset of this phenomenon. The synergistic effects of this regional pattern of activation and electromechanical delay are evidence suggesting kinematic morphology is coded early in the flexion's time course. As to eliminate the effects of this increased voltage, EMG signals that occurred above 60% of

the range of motion were attenuated with a rectangular window. The windowed EMG waveforms (r-EMG) were used in subsequent processes.

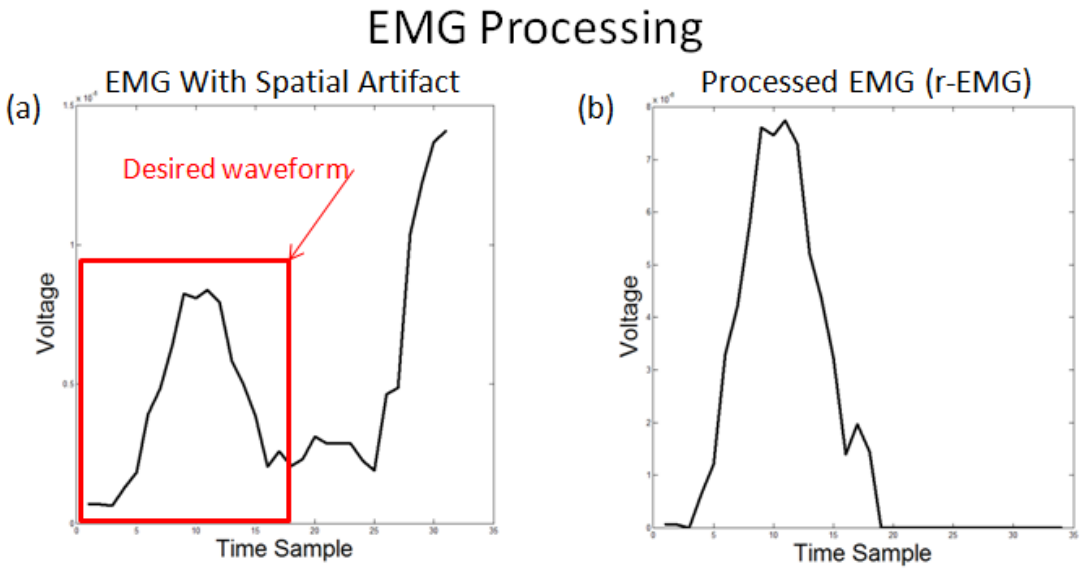

Figure 3: EMG Processing – (a) The desired waveform occurs early in the EMG profile. The spatial artifact is readily observed near full flexion. (b) Completion of EMG processing removes the artifact and leaves the desired waveform in-tact.

B.2. Modeling

Previous work in our lab had shown that spatiotemporal morphology of a single joint trajectory conforms to an array of degenerate waveforms. In this study, I chose to reconstruct global elbow kinematics by the best-fit line (a), sigmoid (b), and concave-down (c) waveforms.

$$m_{i,\chi=a\cdots f}(l,p)=\left\{\begin{array}{ll}\left(\frac{i-p}{l}\right) & a\\ \frac{1}{2}\cdot\left[1+\sin\left(\frac{i-p}{l}\pi-\frac{\pi}{2}\right)\right] & b\\ \left[1-\left(\frac{i-p}{l}\right)^2\right] & c\end{array}\right\}_{\substack{p=0:T-1\\ l=5:T-1}} \quad \text{(Equation 1)}$$

$$\tilde{\theta}_{i\chi}(l,p)=\left\{\begin{array}{ll}0 & 0\le i<p\\ m_{i\chi}(l,p) & p\le i\le p+l\\ 1 & p+l<i<T\end{array}\right\}_{\substack{p=0:T-1\\ l=5:T-1}}. \quad \text{(Equation 2)}$$

[Wininger 2009]

The model waveform, developed from Equation 1 and Equation 2, had to account for variable velocity and stalls observed in between flexions and extensions. A model of a specific kinematic type was identified by iteratively increasing the temporal resolution of the waveform while time-shifting the model across the spatially normalized flexion. Successive comparisons between the normalized flexion data and the model were made

to maximize goodness of fit, as measured by correlation. One-to-one time correspondence was maintained between the performed flexion and the model by adjusting the leading and trailing pads of model waveform.

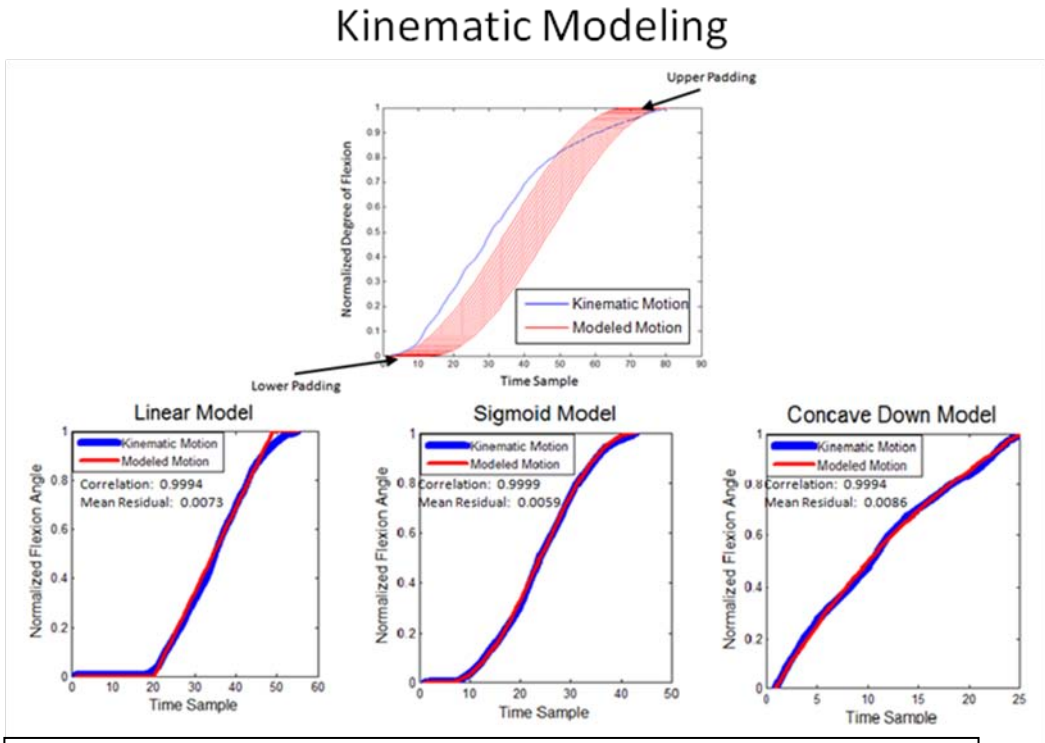

Figure 4: Kinematic Modeling – Spatiotemporal trajectories are reconstructed by a set of three monotonic functions. The optimal model is discerned by a pseudo-convolution that seeks to maximize the correlation between the model waveform and the flexion.

A similar modeling technique was used to reconstruct the processed EMG recordings; a best-fit parabolic trace was identified for each of the EMG recordings (p-EMG). In order to preserve the information content of the EMG amplitude, the waveforms were not normalized. The model amplitude was iteratively adjusted after cycles of iteratively increasing temporal resolution and time-shifting.

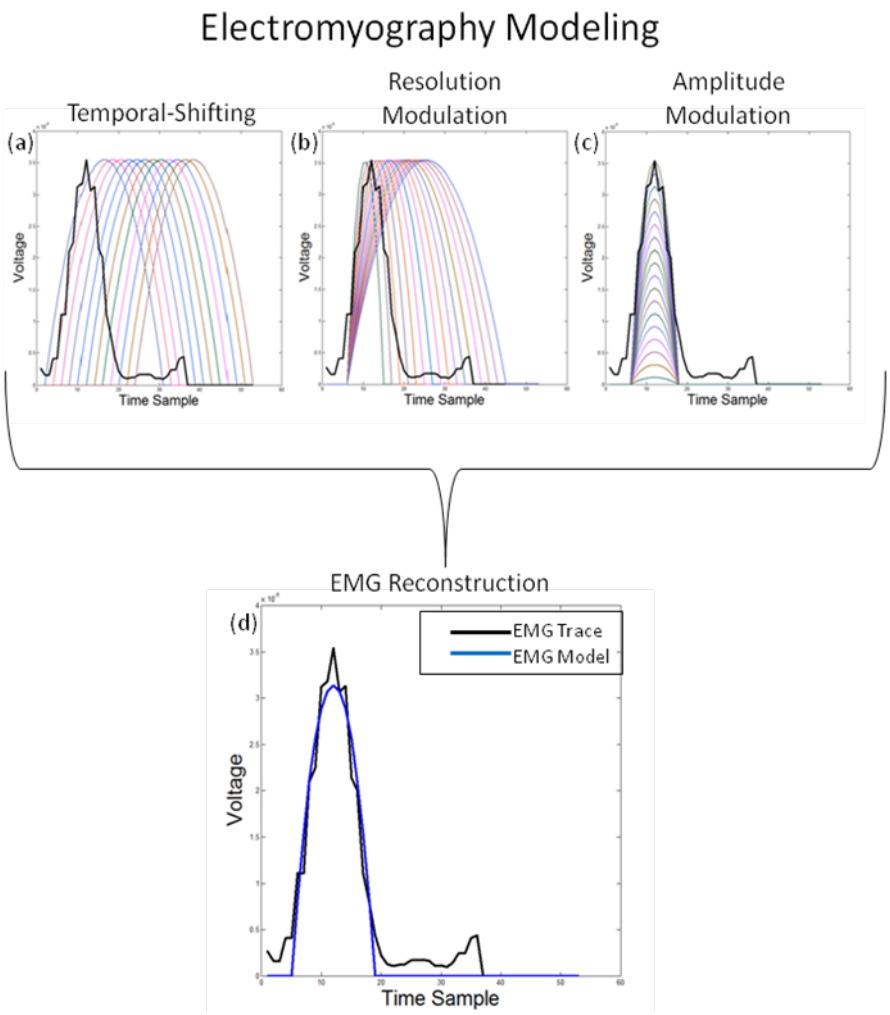

Figure 5: Electromyography Modeling – The algorithm used to identify the best-fit parabolic trace is illustrated. (a) A parabolic waveform of specific temporal resolution and amplitude is compared to the EMG trace after each time-step in an effort to maximize correlation. (b) The temporal resolution is iteratively increased after each cycle of temporal-shifting is completed. (c) The amplitude of the waveform is adjusted after each nested cycle of resolution modulation and temporal-shifting. (d) The nested curve matching algorithm reconstructs the EMG trace with the best-fit parabolic model (p-EMG).

C. Kinematic Characterization

Our ultimate goal was to use r-EMG and p-EMG to independently predict kinematic morphology of self-paced, untargeted elbow flexions. Specifically, I asked the question, do EMG features accurately predict the type of kinematic pattern? Criterion used to classify kinematic type was a threshold based on the correlation between the model and repetition. This goodness of fit criterion was determined empirically by performing a preliminary examination of the data using a random cross validation and remained constant across kinematic types and subjects. A fixed threshold of $r^2 > 0.9979$ was used to identify repetitions that adhered to a kinematic type, whereas departure from a kinematic type was defined as $r^2 < 0.9951$. Model-kinematic trace correlations that fall between 0.9951 and 0.9979 were omitted from classification.

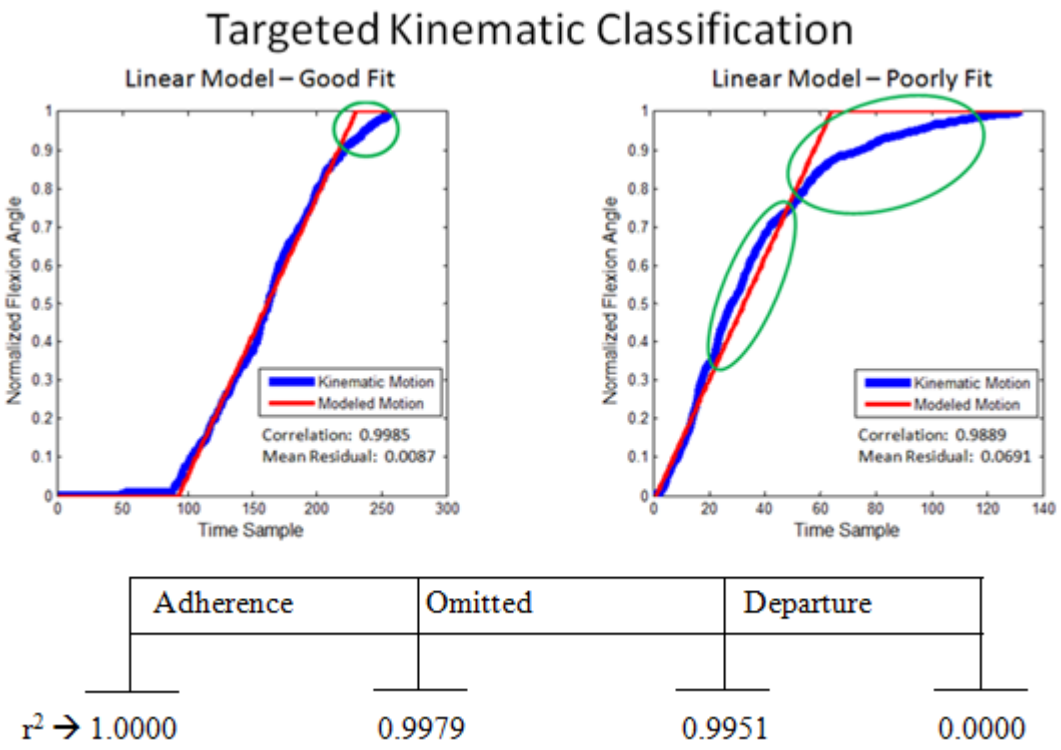

Figure 6: Targeted Kinematic Classification – A repetition that satisfies the adherence criterion (left) nearly coincides with the linear model. Periods of discord between the reconstruction and the kinematic trace yield poor correlation (right). The table depicts the definitions of adherence and departure.

D. Machine Learning

D.1. Feature Extraction

Features, or waveform characteristics, were extracted from r-EMG and corresponding p-EMG. Three broad categories of features were compiled: independent EMG parameters, temporal relationships, and spatial relationships. Independent EMG parameters, including amplitude, mean, standard deviation, and energy (area under the curve (AUC)), were derived strictly from the voltage recorded during the flexion. On the other hand, temporal relationships indicated when an EMG event took place in relation to the period of the flexion. Temporal occurrence of peak EMG and duration of activation were normalized in the time-domain by the duration of the flexion. Spatial relationships, produced by identifying the angular position that coincided with an EMG event, were correlated with specific kinematic landmarks. Spatial relationships included flexion angle at peak EMG and the angular distance traversed while the biceps were activated. Muscle activation was defined as voltage greater than 10 % of the peak EMG amplitude of each repetition.

EMG Feature Set			
Feature		Feature Type	Definition
1.	Amplitude	EMG	Maximum voltage
2.	Mean	EMG	Mean voltage
3.	Standard Deviation	EMG	Standard Deviation Voltage
4.	Energy	EMG	AUC
5.	Peak EMG –Temporal	Time-domain	(Time – peak EMG)/duration flexion
6.	Duration	Time-domain	Time – above 10% amplitude/duration
7.	Peak EMG – Spatial	Spatial	Flexion angle(peak EMG)
8.	Distance Traversed	Spatial	Theta above 10% amplitude

Table 1: EMG Feature Set – Extracted features are listed along with the type of feature and its mathematical definition.

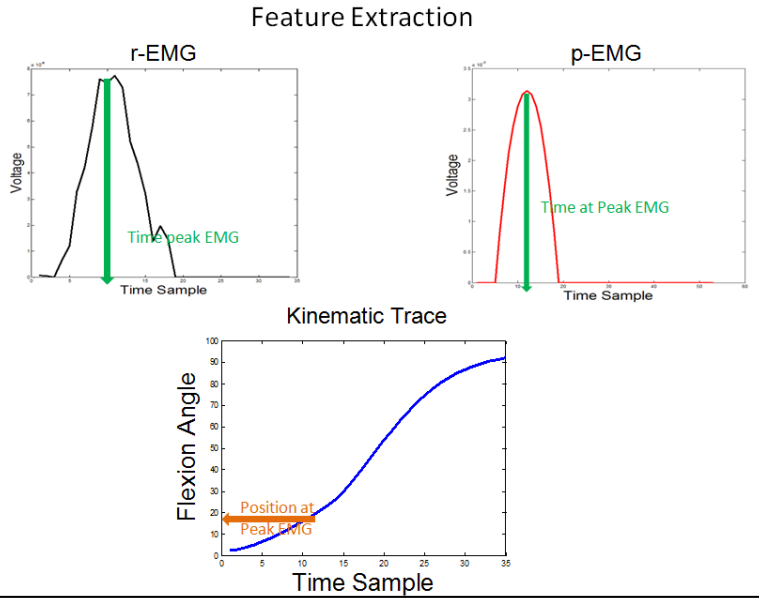

Figure 7: Feature Extraction – Three possible features are extracted from a single event that occurs in the EMG record: the magnitude of the event, the temporal occurrence, and the position in the workspace. Collectively, these features from an assortment of events comprise the feature subspace.

D.2. Feature Reduction

The feature set extracted from the EMG recordings may contain uninformative or redundant features. The presence of these latent features drastically increases the computational power needed to train a supervised learning classifier (each additional feature exponentially increases the volume of the feature hyperspace) [Burges 1998]. Therefore, reducing the feature space to those which contain relevant information was of paramount importance. Principal components analysis (PCA) is a linear transformation that rotates the data in order to elucidate variables, or principal components, that contain the most variation [Semmlow 2004]. Each feature was z-normalized before PCA was performed. A scree analysis of the principal components, as shown in Figure 8, revealed that a vast majority of the variability (up to 95%) can be explained by 3 components. The principal components are highly informative, but extremely difficult to interpret because they are an unknown combination of the variables in the original feature space [Semmlow 2004]. In essence, in order to operate in the original EMG feature space, I needed to identify the number of features that generate the information residing in the principal components. Minimally, 3 features in the original feature space had to be identified; since 3 principal components, which were an unknown combination of an unknown number of original features, were required to explain the variability in the data I needed to identify at least 3 EMG features. Ideal features minimize the within class variance and maximize the difference between classes; the feature space depict each class as a dense packet of data whose centroids are separated by a large distance. Therefore, difference of means tests were used to assess the dimensionality of the data. For each

kinematic type, a comprehensive search was performed that minimized the p-value (maximized difference of means) of every combination of subspaces in feature spaces of iteratively increasing dimensionality. The difference of means tests did not increase in significance as the dimensionality exceeded 3 features (see Figure 9). Instead, the p-values began to increase as more features were included in the feature space. Increased dimensionality would simply increase the training time required without improving the information content of the feature space. Therefore, it was determined that a 3 feature subspace was required for classification.

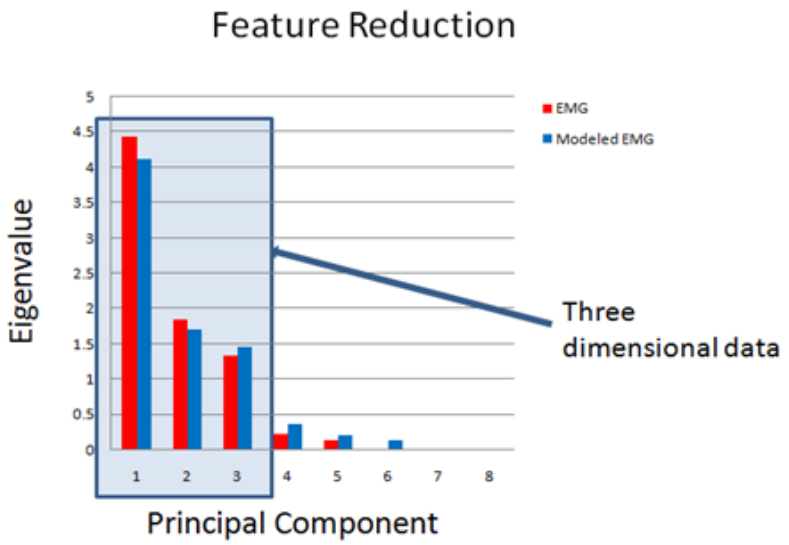

Figure 8: Feature Reduction – Principal Components Analysis (PCA) shows the vast majority of the variability (up to 95%) in the data can be attributed to 3 principal components. The scree analysis depicted here is a sample from a single subject.

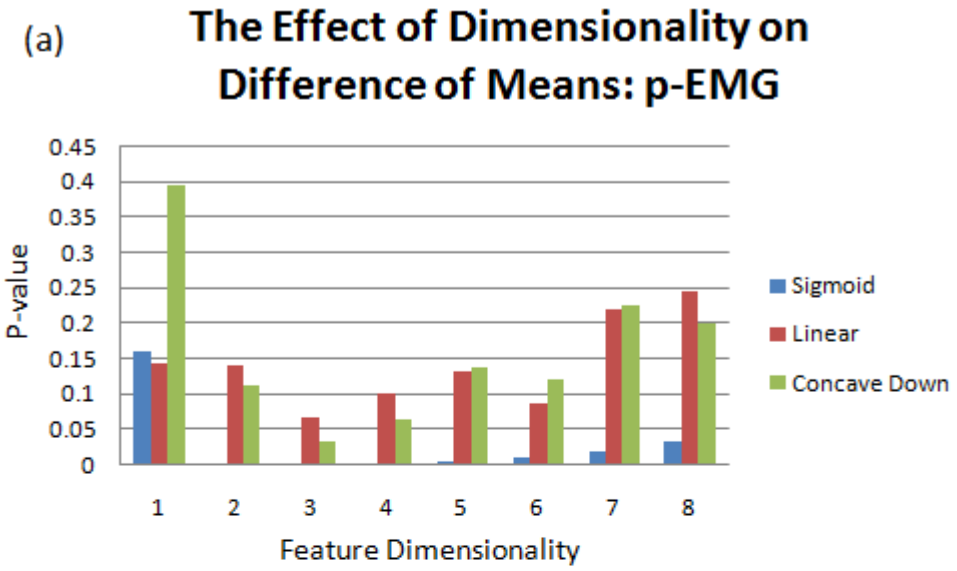

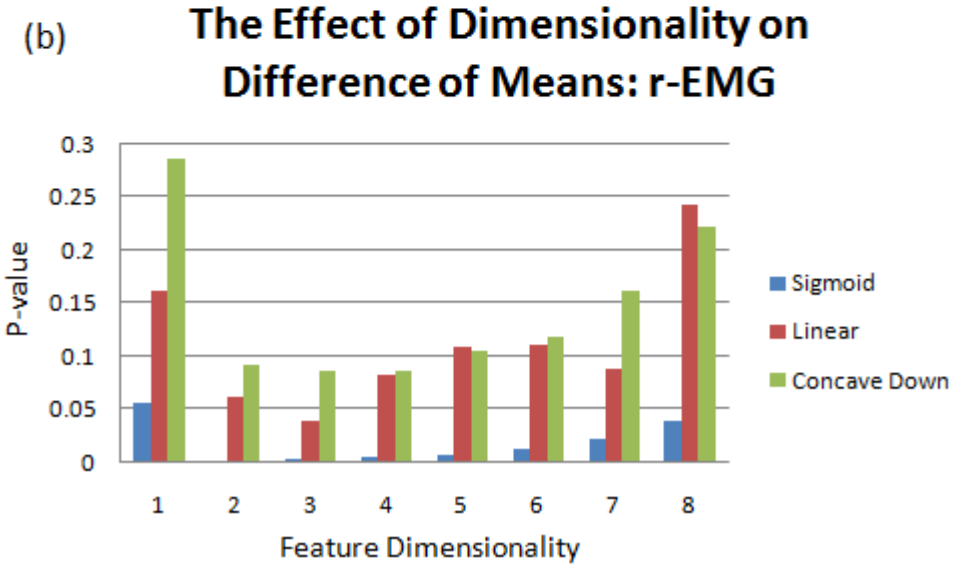

Figure 9: The Effect of Dimensionality on Difference of Means – A multivariate difference of means test is used to probe all possible feature subspaces at each dimensionality. The minimum p-values for the comparisons made within each kinematic type are shown for all dimensions. P-values are minimized in a 3-dimensional feature space. This indicates that increasing the dimensionality further includes redundant or uninformative features. Therefore, a 3 feature subspace was deemed appropriate.

D.3. Feature Selection and Classification

Next, a 3 feature subspace containing the predictive value elucidated by Feature Reduction (Section 2.D.2) had to be identified. My feature selection process can be separated into two distinct sub-processes: identification of potential optimal subspaces and selection of the singular optimal subspace.

Several subspace combinations can be assembled from the octal feature space from Table 1; it was necessary to generate a short list of potential optimal subspaces to make computing time manageable. For each kinematic type, a comprehensive search was performed which discerned the 3 feature subspace that maximally separates the means between the EMG traces from the kinematic adherence group from the kinematic departure group (minimizing p-value). A list of up to 3 potential subspaces was developed because tests of difference in means can be skewed by an EMG wave. Despite thorough processing techniques, it wasn't uncommon to encounter these "rogue" EMG waves that differ vastly from other EMGs that belong to the same group. Consequently, minimal p-value did not necessarily correspond to maximal predictive value, yet I expected minimal p-value is highly correlated to predictive value. One of my potential candidates should yield maximal predictive value as determined by the support vector machines (SVMs).

EMG's capability to predict kinematic morphology was assessed by linear SVMs. Linear boundaries avoid over-fitting and are the preferred decision boundary for Gaussian data [Semmlow 2004]. Each of the subspace candidates were probed with SVMs in a leave-one-out cross validation. This cross validation paradigm tests the

classifier with the only data sample that is excluded during training [Burges 1998]. The classifier was then re-trained while excluding a different point that was used to test the classifier. This cycle continued until all of the data were tested. SVMs were chosen the assess EMG's predictive capabilities because decision boundaries are determined by examining the data located nearest the boundary [Burges 1998]. Consequently, "rogue" EMG waves will have a minimal effect on discerning the decision boundary because they will be located in the extremities of the feature space. SVMs were not used in the preliminary stages of feature selection because of the long computing time required to train the classifiers. Probing a comprehensive list of subspaces with SVMs would have taken an enormous amount of computing time, thereby requiring the multivariate regression discussed above.

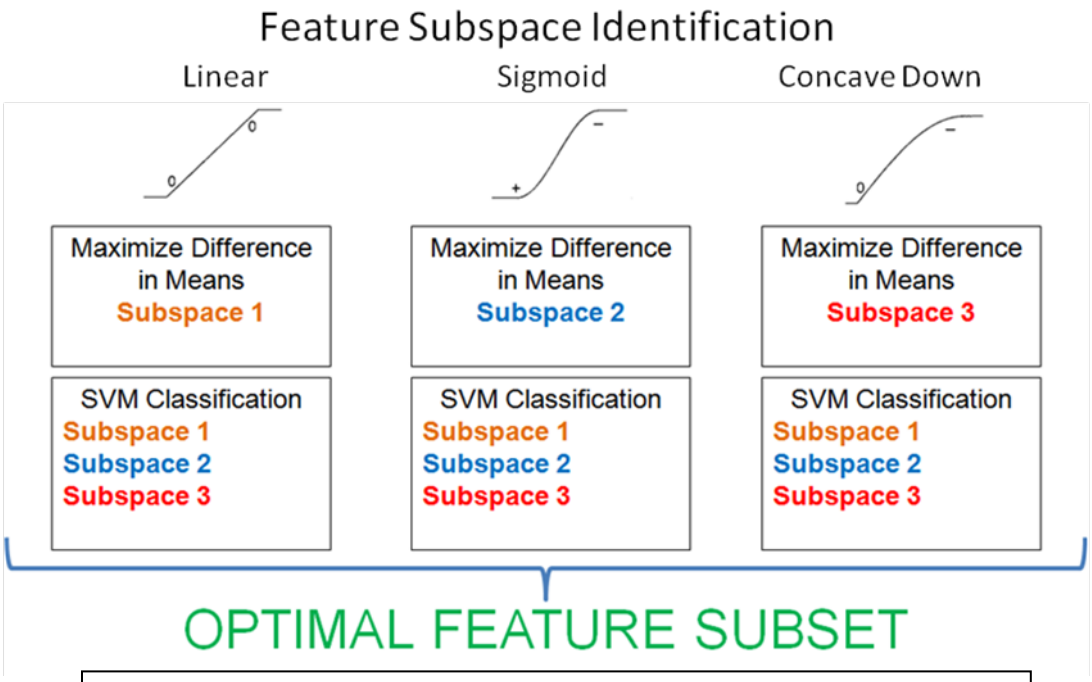

Figure 10: Feature Subspace Identification – The output of multivariate regression yields a potential subspace extracted from each kinematic comparison. A single subspace is identified after examining the output of SVM classification for each subspace performed across kinematic types.

Section 3. RESULTS

Fourteen subjects were recruited for this study, but only 12 met the selection criterion for classification; subjects must have performed at least 5 repetitions that were reconstructed well ($r^2 > 0.9979$) or poorly ($r^2 < 0.9951$) by a corresponding kinematic type. It was common to find subjects who did not meet the selection criterion for all of the kinematic types. Consequently, classification was performed for the cases that contained sufficient repetitions. From the Table 2, it can be seen that only 3 subjects met the kinematic selection criteria for all kinematic types, and the remaining subjects were omitted from at least one classification.

Repetitions Used in SVM Classification						
	Sigmoid		Linear		Concave Down	
Subject	Well Fit Reps	Poorly Fit Reps	Well Fit Reps	Poorly Fit Reps	Well Fit Reps	Poorly Fit Reps
1	21	26	N/A	N/A	24	7
2	N/A	N/A	N/A	N/A	5	9
3	19	13	N/A	N/A	N/A	N/A
4	9	10	N/A	N/A	6	11
5	18	26	N/A	N/A	18	15
6	19	6	N/A	N/A	N/A	N/A
7	13	6	N/A	N/A	N/A	N/A
8	14	16	N/A	N/A	N/A	N/A
9	30	15	13	15	9	6
10	13	13	11	12	6	9
11	N/A	N/A	13	28	N/A	N/A
12	10	52	36	10	37	15
Total	**166**	**183**	**73**	**65**	**105**	**72**

Table 2: Repetitions Used in SVM Classification – The number of repetitions that were used in each binary classification are tabulated. Repetitions that correlated well ($r > 0.9979$) and poorly ($r < 0.9951$) with a given kinematic type are tabulated for each subject. If a subject did not perform at least 5 repetitions that both adhered to and departed from a kinematic type, data were omitted from classification (N/A).

Relevant EMG features were those that could predict the adherence of a spatiotemporal trajectory to a kinematic type. Feature reduction discussed in Section 2.D.2 discerned that a 3 dimensional EMG feature subspace was required for making an adequate binary classification of kinematic type (see Figure 8 and Figure 9). Following feature reduction, the most informative features had to be selected for predicting kinematic morphology. Regression methods probed r-EMG and p-EMG features independently in search of a 3 feature subspace that best predicted kinematic morphology. Thereby, it was possible to identify a unique feature subspace from both EMG modalities for each subject; none of the features were predisposed to selection in the optimal subspace. I was able to conclude that the features were robust across subjects: spatial location of peak EMG[1], temporal occurrence of peak EMG[5], and EMG duration[6] were identified during feature selection more often than the other features (Table 1). Furthermore, there was concordance between the optimal features identified from p-EMG and r-EMG ($r^2 = 0.4514$), as shown in Figure 11(below).

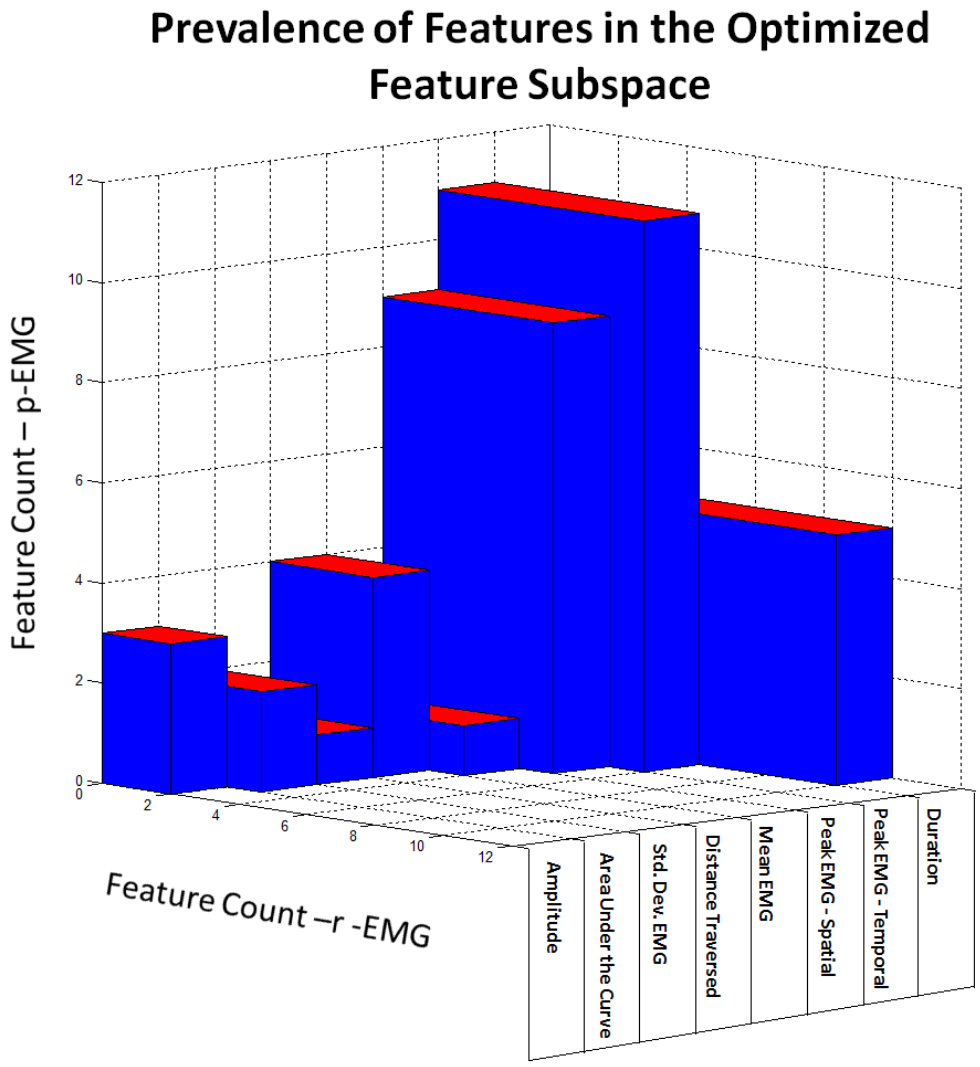

Figure 11: Prevalence of Features in the Optimized Feature Subspace – Duration, temporal occurrence of peak EMG, and spatial location of peak EMG occur in the optimal feature subspace more often than any other feature. There is accordance between p-EMG and r-EMG. Each incremental tally on the "Feature Count" axes represents the inclusion of a specific feature in the optimal feature subspace. Therefore, each feature had a maximum likelihood of 12 identifications (1 for each subject).

The EMG optimal feature subspace contained sufficient information to predict adherence to a kinematic type. For all kinematic types, the mean sensitivity and specificity were observed to defeat chance. Additionally, paired Student's t-tests were

performed to compare the similarity between the performance of p-EMG and r-EMG in predicting kinematic morphology. p-EMG and r-EMG are paired events because p-EMG is a best-fit parabolic trace, and therefore dependent on r-EMG. The t-tests universally concluded there was no significant difference between the p-EMG and r-EMG. A Receiver Operating Characteristic (ROC) analysis, Figure 12, and confusion tables, Figure 13, clearly show EMG's ability to predict kinematic morphology across subjects.

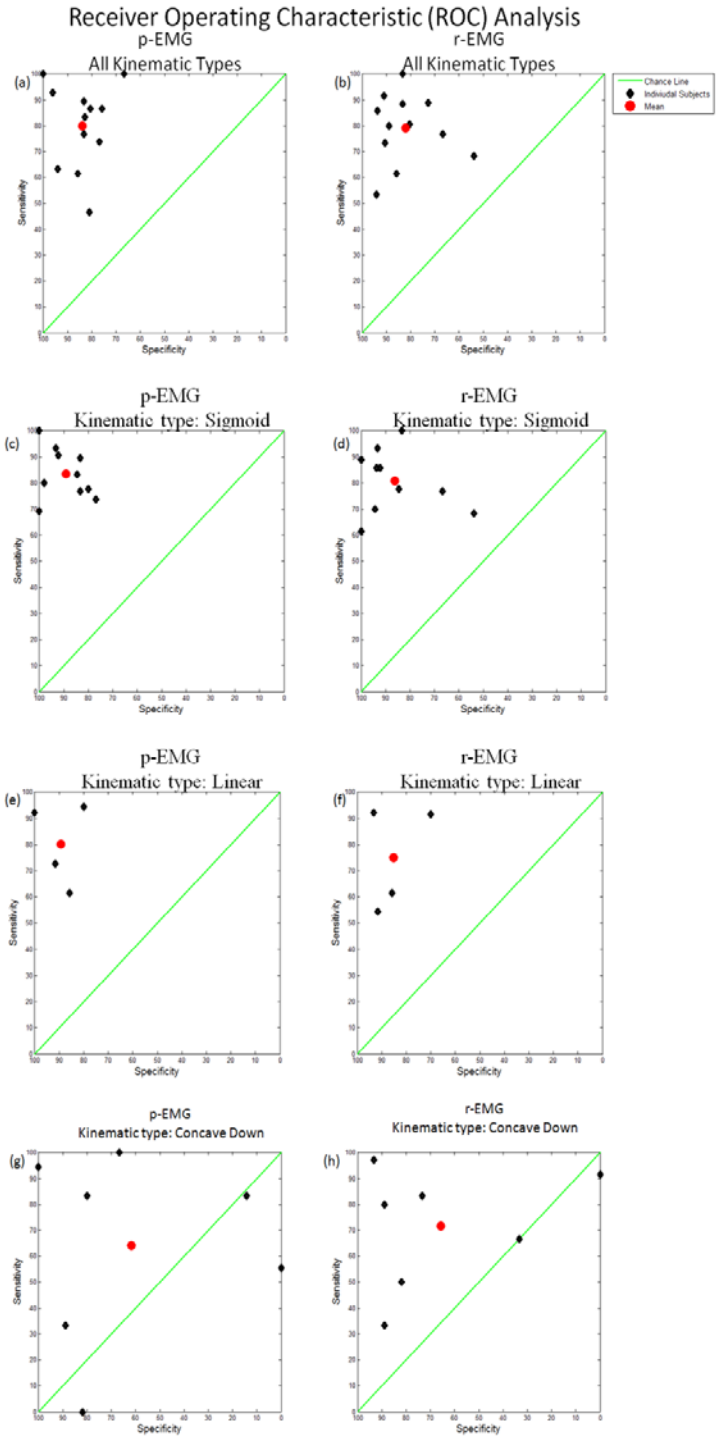

Figure 12: Receiver Operation Characteristic (ROC) Analysis – Results from SVM classification of the p-EMG (left) and the r-EMG (right) for each kinematic type are presented for each subject.

Confusion Analysis of r-EMG and p-EMG

(a)

p-EMG All Kinematic Types		Predicted		
		Positive	Negative	Total
Actual	Positive	82.85%	17.15%	344
	Negative	13.43%	86.57%	320
	Total	328	336	664

(b)

r-EMG All Kinematic Types		Predicted		
		Positive	Negative	Total
Actual	Positive	82.56%	17.44%	344
	Negative	15.31%	84.69%	320
	Total	333	331	664

(c)

p-EMG Kinematic Type: Sigmoid		Predicted		
		Positive	Negative	Total
Actual	Positive	84.94%	15.06%	166
	Negative	8.20%	91.80%	183
	Total	156	193	349

(d)

r-EMG Kinematic Type: Sigmoid		Predicted		
		Positive	Negative	Total
Actual	Positive	82.53%	17.47%	166
	Negative	10.93%	89.07%	183
	Total	157	192	349

(e)

p-EMG Kinematic Type: Linear		Predicted		
		Positive	Negative	Total
Actual	Positive	84.93%	15.07%	73
	Negative	10.77%	89.23%	65
	Total	69	69	138

(f)

r-EMG Kinematic Type: Linear		Predicted		
		Positive	Negative	Total
Actual	Positive	80.82%	19.18%	73
	Negative	13.85%	86.15%	65
	Total	68	70	138

(g)

p-EMG Kinematic Type: Concave Down		Predicted		
		Positive	Negative	Total
Actual	Positive	78.09%	21.91%	105
	Negative	29.16%	70.84%	72
	Total	103	74	177

(h)

r-EMG Kinematic Type: Concave Down		Predicted		
		Positive	Negative	Total
Actual	Positive	83.81%	16.19%	105
	Negative	27.78%	72.22%	72
	Total	108	69	177

Figure 13: Confusion Analysis of r-EMG and p-EMG – The confusion tables include all of the decisions made during SVM classification for p-EMG (left column) and r-EMG(right column).

Statistical Examination of p-EMG versus r-EMG Predictive Value

		Kinematic Type			
		All	Sigmoid	Linear	Concave Down
p-EMG	Specificity Mean (%)	83.86	89.19	89.23	61.66
	Specificity Std. Dev. (%)	9.29	8.59	8.55	38.78
	Sensitivity Mean (%)	80.08	83.42	80.25	64.3
	Sensitivity Std. Dev. (%)	16.32	9.67	15.85	36.71
r-EMG	Specificity Mean (%)	82.02	86.21	85.17	65.66
	Specificity Std. Dev. (%)	12.12	15.02	10.63	35.4
	Sensitivity Mean (%)	79.06	80.83	75.01	71.75
	Sensitivity Std. Dev. (%)	13.3	12.04	19.81	23.19
	Specificity P-value	0.5881	0.5921	0.5638	0.8840
	Accepted Hypothesis	Null	Null	Null	Null
	Sensitivity P-value	0.7730	0.6020	0.6939	0.6580
	Accepted Hypothesis	Null	Null	Null	Null

Table 3: Statistical Examination of p-EMG versus r-EMG Predictive Value – The sensitivity/specificity numbers presented here weight each subject equally, and are reflective of the ROC analysis (Figure 12). Paired t-tests compared sensitivity and specificity from the model trace and EMG trace to determine whether the two modalities predict kinematic morphology similarly. The null hypothesis stated the means of p-EMG and r-EMG were not significantly different ($p \geq 0.05$). The alternate hypothesis stated the means of p-EMG and r-EMG would yield significantly different predictive values ($p < 0.05$). In all cases, the predictive value were not significantly different.

Section 4. DISCUSSION

The results herein suggest that the initial neural command, measured by EMG, is predictive of certain kinematic morphology, which is characterized by a few statistically independent trajectory types. Both EMG modalities, r-EMG and p-EMG, successfully predicted kinematic morphology with high sensitivity and specificity across kinematic types. Confusion analysis revealed r-EMG predicted kinematic morphology with a sensitivity of 82.56% and specificity of 84.69%. The predictive value of a parabolic envelope of r-EMG yielded similar with sensitivity of 82.85% and specificity of 86.57%. There was no statistical difference between the predictive value of p-EMG and r-EMG. Furthermore, the features most often selected for classification were robust across subjects and EMG modalities.

The consistency in EMG predictions implies there was degeneracy in motor planning across subjects. Strict adherence parameters in the kinematic domain only permitted repetitions that nearly coincided with the kinematic model to be used in subsequent analyses. This selective group of repetitions had a highly invariant kinematic morphology. Therefore, it is nearly impossible to associate a repetition with a subject; within subject and across subject variation is similar after imposing the adherence criterion.

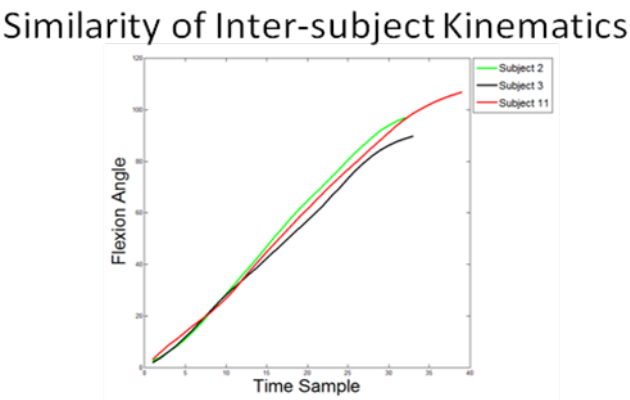

Figure 14: Similarity of Inter-subject Kinematics – Sample flexions adhering to sigmoid morphology from three different subjects. The repetitions nearly coincide and it is difficult to discern that the flexions were performed by different subjects.

As hypothesized, invariance in kinematic morphology was reflected in the bioelectric domain. This was surprising because of EMG's notoriously stochastic nature and the increased degrees of freedom in the nervous system. Yet EMG's predictive value persisted across subjects. The relatively tight distribution of individual's sensitivity and specificity about the mean echoed the invariance in the kinematic domain. Furthermore, the features selected in the optimal subspace were robust across subjects. The repetitive identification of temporal occurrence of peak EMG, spatial location of peak EMG, and duration of EMG as optimal features implied there is parametric degeneracy in the EMG. Degenerate information in the EMG would fit perfectly with the central dogma of trajectory analysis; single joint trajectories have routinely been reported to approach a linear path with a bell-shaped velocity profile [Flash& Hogan 1985; Rohrer et al. 2002].

The similarity of goodness of fit across kinematic types confined predictions to adherence to a single morphology. Predictions can't be made across kinematic types because adherence to waveform morphology was not mutually exclusive; repetitions

could be reconstructed well by multiple kinematic models. Totally, there were 486 repetitions matched to at least a single trajectory type (r^2>0.9979), and 159 of these repetitions were reconstructed well by multiple kinematic types.

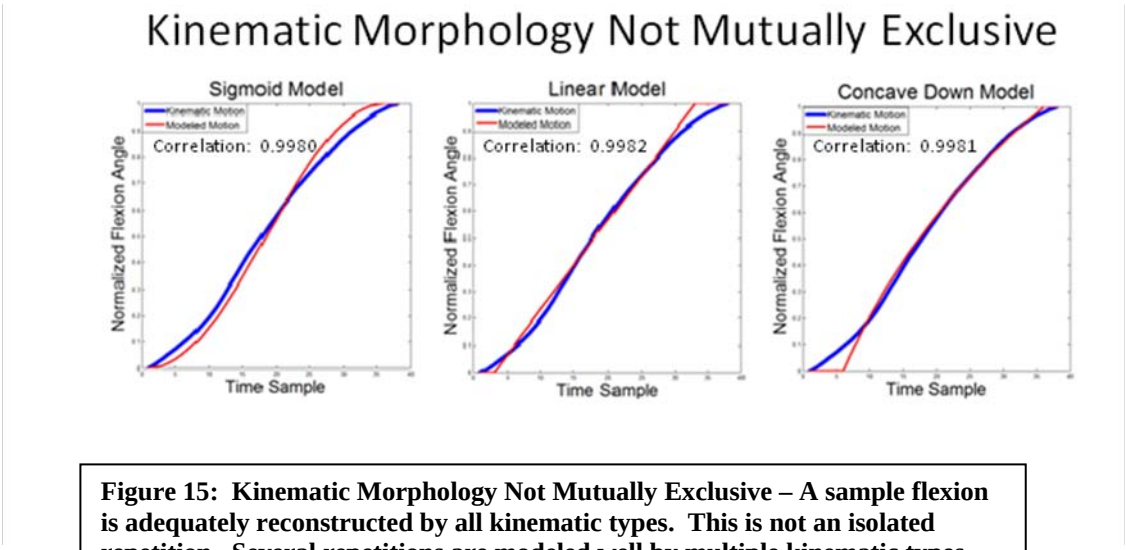

Figure 15: Kinematic Morphology Not Mutually Exclusive – A sample flexion is adequately reconstructed by all kinematic types. This is not an isolated repetition. Several repetitions are modeled well by multiple kinematic types.

The differences in correlation between the kinematic model and actual subject motion were considered to be negligible above r^2=0.9979. Any differences in modeling accuracy that occur above the correlation threshold were attributed to local motor phenomena and/or physiological noise instead of varying global morphology. It would be futile to attempt predicting kinematics across trajectory types because of the propensity of encountering repetitions that are well fit by multiple models. The similarity of goodness of fit across kinematic types created ambiguity to the assignment of a repetition to a single kinematic type. Which kinematic type would a repetition depicted in Figure 15 belong to? A between-kinematic types comparison requires repetitions that were

reconstructed well by a single kinematic type and poorly modeled by all other morphologies; only 38 of these repetitions exist in all of the recorded data.

Global arm flexion kinematic morphology was successfully predicted from the EMG that occurs early in the development of the motion. EMG records were windowed to the time-course that occurred within the first 60% of the angular distance traversed. Thus, EMG records were modeled by one parabola instead of a biphasic model. Despite subsequent predictions of kinematic morphology relying entirely on the truncated EMG waveform, trajectory type was predicted with high sensitivity and specificity. The substantial predictive value concentrated in the windowed domain of the EMG signal can be partially explained by electromechanical delay and accelerative patterns observed in the kinematics. Electromechanical delay is predicated on the notion that muscle contractions lag behind the neural command. So far, the time delay has been poorly quantified, and seems to be dependent on the velocity of contraction [Sarre & Lepers 2007]. An EMG trace truncated at 60% of the range of motion contained information about the kinematics occurring beyond the spatial window. Electromechanical delay coupled with typical kinematic events resulted in classification of high sensitivity and specificity. Each flexion is marked by a period of acceleration at the onset of the motion near full extension followed by a period of relatively constant velocity and terminating with a stopping period of deceleration. The period of constant velocity occupies the vast majority of flexions time trace, which implies adherence to a kinematic type is largely affected by the accelerations experienced at the tails of each flexion. EMG segments corresponding to these accelerative events are thereby extremely valuable in proper

classification. My EMG processing didn't include the data that correspond to the deccelerative pattern near full flexion, so I relied heavily on the flexion's initial acceleration. The absence of this information did not impact predictions to linear or sigmoid patterns because of the symmetric periods of acceleration in the kinematic trace. The noticeable drop-off in predicting concave down trajectories was possibly due to inadequate information in the EMG. I had no way of accounting for the trace's constant deceleration; this is due to an exclusion of either triceps data or the removal of the EMG traces that correspond to the last 40% of the motion. Triceps EMG were recorded, however due to poor SNR, a robust depiction of muscle activation could not be generated.

A primary objective of this study was to examine the similarity of the information content of r-EMG and p-EMG. The two signals, which were extracted from the same raw EMG, corroborated well in predicting global arm function kinematics rendered from the same features. Duration, spatial location of peak EMG, and temporal occurrence of peak EMG were the most frequently used features in the optimal subspace. These features resulted in a strikingly similar pattern of predictive value. There was no statistical difference between the sensitivity or specificity ($p = .05$) in the traces' ability to predict the selected kinematic types. In fact, p-EMG performed marginally better than r-EMG during classification. Further dissection of the accordance between the traces revealed that they yielded the same prediction 87.80% of the time. The synergy between the similar optimal feature subspaces and predictive values is convincing evidence that p-EMG replicates the r-EMG's ability to predict global morphology, as depicted in the

Figure 16 (below). However, this does not indicate that p-EMG reconstructs r-EMG. p-EMG represents a smooth, low-pass filtered model of r-EMG. r-EMG may contain layers of information in the high-frequency domain that I did not considered. A bulk of this information may reside in the residual waveform that was masked out in this study. This residual waveform is derived by subtracting p-EMG from r-EMG. This residual waveform may correlate to short periods of accelerations observed throughout a flexion. Further investigation is necessary to discern the relevance of the remainder of the EMG waveform.

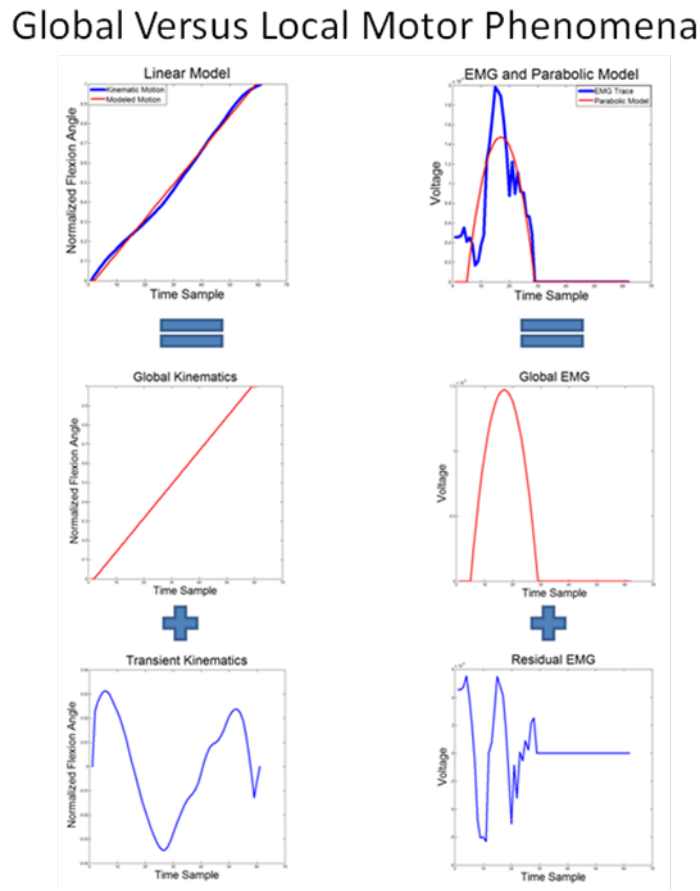

Figure 16: Global Versus Local Motor Phenomena – Distinction between global and local effects is depicted. The panels in the left hand column display the parametric reconstruction superimposed over the performed motion, the global flexion morphology, and the aspect of kinematics that were not accounted for (top to bottom). The EMG correlates of each of these is displayed in the right hand column. This study focused entirely on the global flexion motor phenomenon. Future studies should investigate the characteristics present in the Residual EMG that correlate to Transient Kinematics (bottom row).

Frequently identified optimal features limit EMG models to sloped waveforms. Historically, EMG had been modeled by both rectangular waves and impulse functions [Raasch et al. 1997; Neptune & Hull 1998]. All of the optimal features can't be extracted from these waveforms. Impulse functions are zero everywhere except the time point that coincides with peak EMG amplitude. In other words, the instantaneous nature of the

wave is that it does not have duration. By contrast, square waves have a non-zero rise to peak voltage enduring the period of activation. In this case, peak EMG is not a single point measurement as in the parabolic model. Therefore, temporal occurrence and spatial location of peak EMG can't be discerned accurately. Although a comprehensive feature set can be extracted from any sloped waveform, comprehensive feature sets from sloped waveforms do not correspond to similar informative content. A model waveform that poorly reconstructs EMG can have a plethora of features extracted from it, but the classification will not concur with the predictions made by EMG. In a similar sense, parabolic reconstructions are relatively accurate representations of EMG; my predictions of kinematic morphology from p-EMGs yielded good results.

Early phase of EMG in relation to the angular position in the workspace seems to have a deterministic effect on the spatiotemporal trajectory. Inclusion of spatial location of peak EMG in the optimal feature subspace may reflect proprioceptive feedback. Proprioception is the ability to sense the relative position and orientation of body parts in the extracorporeal space via neural feedback [Widmaier et al. 2006]. Reflexive real-time tuning of arm position using proprioceptive trajectory formation may explain subjects' subscription to select degenerate morphologies [Wininger et al. 2009]. Each individual may have unique intrinsic motor functional characteristics where a specific flexion angle/trajectory is obtained as a result of their unique neural signal transduction. Factors that may govern unique neural transduction patterns may include the musculature's ability to recruit afferent and efferent neurons and individual's musculoskeltal morphology (i.e. age, gender, functional mass of a specific limb under investigation,

etc.). Specifically, my findings demonstrated maximal activation of the biceps at a specific flexion angle predisposed a flexion's adherence to a certain kinematic type or types. Since proprioception/kinesthesia is an acquired ability, the degree of varying effects from feedback on a repetition-to-repetition basis should be relatively small with respect to a parametric analysis. However, variability in the execution of highly practiced tasks has been shown to be substantial [Bernstein 1967]. The fact that each individual's arm movements adheres to a small set of degenerate trajectories was consistent with previous findings which showed similar results where a few kinematic phenotypes were capable of describing a large number of healthy subjects' functional patterns at the elbow [Wininger et al. 2009].

Section 5. SUGGESTIONS FOR IMPROVEMENT

The fidelity of our EMG signal can be improved significantly by recording multiple channels of data from the biceps. Features extracted from some traces were several standard deviations away from the group mean. Anomalous EMG traces reflect either increased bioelectric activity or spurious noise. These erroneous EMG recordings may be due to numerous reasons that affect the affinity of the EMG electrode to the skin including, but not limited to, temporary shifting of the electrode, increased surface moisture which affects the impedance of the conductor pads, or shifting of the skin itself. Probing the muscle with several electrodes and analyzing the signals in parallel or averaging them would attenuate erroneous measurements from any single channel. Improving signal fidelity by invasive EMG, which uses subdermal or subcutaneous needles, accompanied by near infrared spectroscopy would facilitate a higher resolution prediction of kinematics. The data acquisition modality implemented in this study had good features such as portability, slim form-factor, convenient connectivity, compatibility to various analytic tools, and low cost. However, the experimental infrastructure resided in the moderate end of the power range in terms of signal acquisition specifications. Therefore, more robust signal processing coupled with improved hardware may permit loosening of the stringent goodness of fit parameters, thereby passing more repetitions into the machine learning process. Furthermore, future studies could consider different modalities of acquiring kinematic data, such as an accelerometer, motion capture system, etc.

Reciprocal muscle actions should be included in further analyses. This study operated under the presumption that the biceps were the major contributor to the development of a flexion. However, periods of triceps activity or inactivity is also important to controlling kinematic morphology. The characteristic deceleration in a concave-down trace may be attributed to increased triceps activity rather than biceps activity. Our diminished ability to predict conformity to a concave-down model versus the other kinematic types may be corrected by the inclusion of triceps activity.

The observed drop-off in predicting adherence to a concave-down model may also be remedied by improving processing and modeling techniques. EMG traces were windowed because of the large increase in voltage near full flexion. The inclusion of the EMG time-course removed by windowing may shed light on the accelerations occurring near full flexion. Bisecting flexions, both in the kinematic and bioelectric domains, according to a spatial parameter would enable the large voltages near full flexion to be included in further analyses without attenuating informative content in the low-voltage time course that occurs near full extension. In essence, both arm kinematics and EMG would be parsed into a time-matched ‘near extension’ and ‘near flexion’ phases, which are distinguished by a spatial parameter. Such data processing would enable analyses that examine the entire EMG trace as two distinct segments without any information loss.

Subsequent investigations should correlate the EMG to the short periods of acceleration that occur throughout a motion. This study determined that a parabolic reconstruction of EMG contains sufficient information to predict the global kinematic morphology of elbow flexions. However, no attempt was made to qualify the slight

departures of a kinematic trace from the kinematic model. As discussed earlier, EMG and kinematic residual waveforms can be generated by subtracting the reconstruction from the trace. If the residual EMG wave can predict residual kinematics, then a comprehensive reconstruction of a kinematic trace would be developed from the EMG.

Findings from this study could be applied to rehabilitation engineering if a real-time classification algorithm is developed to implement a similar kinematic predictor in a myoelectric prosthetic device. Current prosthetic devices detect the initial onset of user volition and develop monotone movements that may not reflect the desired kinematics. The premise of this study was to examine the EMG during self-paced, untargeted reaching tasks, which are the most typical, natural elbow articulations. A post-hoc prediction of kinematic morphology was made here; in its current form, adoption of this software in a myoelectric device would result in a large lag time between the user's volition and the actuation of the prosthetic motors. Training time can be reduced significantly if the device learns in real-time with each successive repetition. After sufficient training, device operation would mimic a fully functional, life-like, elbow, which is the ultimate goal in the prosthetic assistive device industry.

Section 6. CONCLUSIONS

This study is the first successful application of EMG to a self-paced, untargeted, autonomous reaching task. Until now, EMG investigations of the upper limb have been restricted to isometric contractions, ballistics motions, and tracked motions. These exercises are conducive to EMG analysis because of a characteristically large rise in muscle activation, which is beneficial to SNR quality. However, these exercises do not reflect life-like kinematics exhibited during self-paced reaching tasks. Our understanding of motor control will be greatly enhanced when a comprehensive depiction of typical kinematics can be resolved from EMG.

I successfully predicted the global morphology of a self-paced flexion from parabolic reconstructions and EMG traces. Correlating EMG to resulting kinematics instead of individual muscle forces that generate kinematics is a departure from the conventional strategy of predicting muscle force from EMG. Elbow kinematics is a well studied phenomenon, and I relied heavily on the degeneracy of kinematic traces in a theoretical parametric space. Both p-EMG and r-EMG were able to predict adherence to a kinematic morphology similarly. Moreover, the two modalities incorporated similar optimal feature subspaces. These similarities signified the parabolic traces contain the information used by the EMG to code for kinematic morphology. Furthermore, the EMG coding was robust across subjects. Robust optimal features coupled with the similar prediction accuracy across subjects indicated there is some degeneracy in the motor plan. This work can be substantially improved to better elucidate EMG characteristics in an attempt to improve our understanding of human motor control. In this study, a

pioneering notion has been proposed that EMG correlates to kinematics during a typical upper arm retrieval task. However, I have certainly not explored the vastness of this unique point of view. This is the beginning of a fresh outlook of EMG and its applications, which is a suggestion as to a new methodology of investigating untouched aspects of human motor control.

Section 7. REFERENCES

Abend, W., Bizzi, E., Morasso, P. Human arm trajectory formation *Brain* **105**: 331-348, 1982.

Adee, S. The revolution will be prosthetized *IEEE Spectrum* **46(1)**: 44-48, 2009.

Bernstein, N. *The Coordination and Regulation of Movements*, 1976.

Burges, C. J.C. A tutorial on support vector machines for pattern recognition *Data Mining and Knowledge Discovery* **2**: 121-167, 1998.

Camilleri, M.J., Hull, M.L. Are the maximum shortening velocity and the shape parameter in a Hill-type model of whole muscle related to activation? *Journal of Biomechanics* **38**: 2172-2180, 2005.

Camilleri, M.J., Hull, M.L., Hakansson, N. Sloped excitation waveforms improve the accuracy of forward dynamic simulations *Journal of Biomechanics* **40**: 1423-1432, 2006.

Doheny, E.P., Lowery, M.M., FitzPatrick D.P., O'Malley, M.J. Effect of elbow joint angle on force-EMG relationships in human elbow flexor and extensor muscles *Journal of Electromyography and Kinesiology* **18**: 760-770, 2008.

Feng, C.J., Mak, A.F.T. Three-dimensional motion analysis of the voluntary elbow movement in subjects with spasticity *IEEE Transactions on Rehabilitation Engineering* **5(3)**: 253-262, 1997.

Flash, T., Hogan, N. The coordination of arm movements: An experimentally confirmed mathematical model *The Journal of Neuroscience* **5(7)**: 1688-1703, 1985.

Georgopoulos, A.P., Kalaska, J.F., Massey, J.T. Spatial trajectories and reaction times of aimed movements: Effects of practice, uncertainty, and change in target location *Journal of Neurophysiology* **46**: 725-743, 1981.

Koo, T.K.K., Mak, A.F.T., Feasibility of using EMG driven neuromuscloskeletal model for prediction of dynamic movement of the elbow *Journal of Electromyography and Kinesiology* **15**: 12-26, 2005.

Morasso, P., Mussa-Ivaldi, F.A. Trajectory formation and handwriting: A computational model *Biological Cybernetics* **45**: 131-142, 1982.

Neptune, R.R., Hull, M.L., Evaluation of performance criteria for simulation of submaximal steady-state cycling using a forward dynamic model *Journal of Biomedical Engineering* **120**: 334-341, 1998.

Raasch, C.C., Zajac, F.E., Baoming, M., Levine, W.S. Muscle coordination of maximum-speed pedaling *Journal of Biomechanics* **30(6)**: 595-602, 1997.

Rohrer, B., Fasoli, S., Hermano K. I., Hughes, R., Volpe, B., Frontera W. R., Stein, J., Hogan, N. Movement smoothness changes during stroke recovery *The Journal of Neuroscience* **22(18)**: 8297-8304, 2002.

Sarre, G., Lepers, R. Cycling exercise and the determination of electromechanical delay *Journal of Electromyography and Kinesiology* **17**: 617-621, 2007.

Semmlow, J. *Biosignal and Biomedical Image Processing: MATLAB-based Applications*, 2004.

Suzuki, M., Yamazaki, Y. Velocity-based planning of rapid elbow movements expands the control scheme of the equilibrium point hypothesis *Journal of Computational Neuroscience* **18**: 131-149, 2005.

Widmaier, E.P., Raff, H., Strang, K.T. *Vander's Human Physiology: The Mechanisms of Body Function*, 2006.

Wininger, M.T., Kim, N-H., Craelius, W. Accurate feature extraction from curve-fitted trajectories *Journal of Biomechanics*, submitted (2009).

Wrbaskic, N., Dowling, J.J. Ballistic muscle mechanisms determined using an EMG-driven model *Journal of Electromyography and Kinesiology* **16**: 32-41, 2006.